scientific reports

Check for updates

OPEN

Synthesis and characterization of biobased capsules formed from interpenetrating networks of alginate and poly(ethylene glycol) for the encapsulation of blue dye

Yasmin Kabalan[1], Bartosz Tylkowski[1,2,3], Silvia De La Flor[4], Marta Giamberini[1] & Xavier Montané[5]✉

Encapsulation technologies have been utilized in laundry detergents mainly as formaldehyde-based capsules which are commonly used to encapsulate active compounds like fragrances, bluing agents and fluorescent whitening agents. Nevertheless, formaldehyde derived materials are toxic, carcinogenic, and non-biodegradable leading to an increase in the microplastic pollution in oceans and consequently harming the marine life. Therefore, the researchers are currently tending towards the replacement of these components by biobased ones. In this work, we present the synthesis of capsules with more than one shell using biodegradable polymers to replace these materials. Moreover, the blue dye used in laundry detergent industry was successfully encapsulated in biodegradable capsules formed by an interpenetrating network of alginate and poly(ethylene glycol) diacrylate (PEGDA) prepared using different conditions. Besides, the capsules were characterized to study their chemical, morphological, thermal, and mechanical properties, to evaluate their water solubility, and to determine how the composition and the preparation methods can affect their properties. The novelty of this system lies in evaluating how modifying a previously reported system using poly(ethylene glycol) dimethacrylate (PEGDMA) and alginate as shells –achieved by replacing the PEGDMA diacrylic monomer with PEGDA– affects the morphology and properties of the resulting capsules. It has been shown that the capsules with PEGDA exhibited improved thermal and mechanical properties compared to the previously described system, which could make them more suitable for their intended applications.

Since the 1950s, encapsulation technologies have been widely developed due to the great advantages they present. Encapsulation, which is defined as the enclosing of a core material by a layer or shell, is being used in different industrial sectors such as adhesives[1,2]pesticides[3]medicines[4]food packaging[5]phase change materials[6]fragrances[7] or textile[8] among others. The fact of being able to wrap a compound with a shell allows it to be protected from external stimuli for long periods of time (for example from oxidation caused by sunlight or moisture), in addition to let a controlled release of the encapsulated material[9–11].

One of the industries in which the encapsulation of compounds has a crucial role is that of detergents[12,13]. Laundry detergents are crucial commodities that are expected to generate $ 242.94 billion by 2029[14]. Actually, the encapsulation of distinct bleaching agents (inorganic compounds like hypochlorites or organic compounds such as fluorescent whitening agents) is explored to clean clothes and other textile materials[15].

Formaldehyde-based shells are the industry standard for these types of applications because they provide durability and excellent chemical and mechanical properties[16,17]. Despite these advantages, the drawbacks associated with the use of formaldehyde cannot be ignored: it is carcinogenic, toxic and non-biodegradable[18,19].

[1]Department of Chemical Engineering, Universitat Rovira i Virgili, Av. Països Catalans 26, 43007 Tarragona, Spain. [2]Eurecat, Centre Tecnològic de Catalunya, Unitat de Tecnologia Química, C/ Marcel·lí Domingo 2, Tarragona 43007, Spain. [3]Faculty of Health Science, Department of Clinical Neuropsychology, Nicolaus Copernicus University in Toruń, Collegium Medicum in Bydgoszcz, ul. Skłodowskiej Curie 9, 85-094 Bydgoszcz, Poland. [4]Department of Mechanical Engineering, Universitat Rovira i Virgili, Av. Països Catalans 26, 43007 Tarragona, Spain. [5]Department of Analytical Chemistry and Organic Chemistry, Universitat Rovira i Virgili, C/Marcel·lí Domingo 1, 43007 Tarragona, Spain. ✉email: xavier.montane@urv.cat

Moreover, the slow degradation of these non-biodegradable capsules once they are released in the environment makes them one of the main causes of the formation of microplastics, which accumulation has a long-term negative effect on ecosystems and on the human health[20]. As evidence of the high risk associated to microplastics, Charlton-Howard et al. reported a study in which a disease only caused by the ingestion of plastics affected seabirds[21]. As far as human health is concerned, Palmer and coworkers recently demonstrated that different polymers were found in human vein tissues[22].

For this reason, governments around the world are taking steps to restrict microplastics. For instance, the Registration, Evaluation, Authorisation and Restriction of Chemicals (REACH) of the UE has lately approved restricting intentionally-added microplastics in products, which is a key step in reducing the plastic pollution[23]. Thus, researchers focus nowadays on the development of capsules using biobased materials that can be extracted from natural resources such as biopolymers and proteins[24,25].

Therefore, natural polymers are an attractive opportunity to design capsule shells with enough strength and durability that could be employed to encapsulate bleaching agents. Chitosan and alginate are natural and non-toxic biopolymers that have the ability to crosslink in the presence of different ions to form hydrogels. As an example, the chemical structure of α-L-guluronate (G) and β-D-mannuronate (M) residues present in sodium alginate and the crosslinking of alginate chains by calcium ions is shown in Fig. 1a and b. Furthermore, the incorporation of other easily crosslinkable monomers into the formulation, such as those derived from acrylic compounds, allows obtaining composites with more crosslinked networks. For example, polyacrylic acid (PAA) has been used to prepare systems which could deliver drugs depending on pH. For instance, chitosan crosslinked with PAA was used as a hydrogel to deliver antibiotics[26].

In our previous paper, Kabalan et al. presented the design of biodegradable capsules based on alginate hydrogel composites for the encapsulation of blue dye[27]. A careful selection of the diacrylic monomer based on poly(ethylene glycol) was performed in that work, based on their ability to polymerize upon UV light irradiation. Indeed, while PEGDMA gave rise to well-formed capsules, in the previous study, PEGDA was discarded since it polymerized phase-separated from gelled alginate and did not produce an interpenetrating network. Nevertheless, this could be also a consequence of the monomer different molecular weights and resulting solubility in water: 600 g/mol in case of PEGDMA vs. approximately 250 g/mol in the case of PEGDA. The previously synthesized alginate-based capsules, which shell was constituted by ionically crosslinked alginate by Ca^{2+} ions and a poly(ethylene glycol) network, were widely characterized, thus proving that they present suitable mechanical and thermal properties for the applications they were conceived for.

Actually, PEGDA can be considered an interesting alternative to PEGDMA for its higher chemical reactivity, which ensures polymerization completion and lower toxicity of the final material (Fig. 1c,d)[28]. Therefore, in the present study, we investigated the effect of PEGDA monomer chain length in the preparation of composite capsules. In contrast to the previously tested low molecular weight PEGDA (M_n (PEGDA) ≈ 250 g/mol), using PEGDA with a longer poly(ethylene glycol) chain (M_n (PEGDA) ≈ 520 g/mol) led to the formation of capsule shells consisting of an interpenetrating network of alginate and poly(ethylene glycol) (Fig. 1e). This was attributed to the water solubility of this high molecular weight monomer[29,30].

Hence, in this article we describe the encapsulation of a blue dye being used in the laundry detergent sector in macrocapsules based on alginate-poly(ethylene glycol) hydrogel composites using high molecular weight PEGDA as starting diacrylate monomer following the previously reported procedure[27]. An extensive characterization of these capsules (chemical composition, morphological, mechanical and thermal properties) allowed to detect differences between the capsules based on PEGDA and those based on PEGDMA. Furthermore, the evaluation of the water solubility of composite capsules prepared using high-molecular weight PEGDA has been also investigated and compared with the water solubility of the previously synthesized alginate-based capsules.

Materials and methods

Materials

Sodium alginate (Viscosity (1% in water; 20 °C): 350–550 mPa.s; MW: 10,000-600,000 g/mol) was purchased from Panreac ITW Reagents (Panreac Química SLU, Castellar del Vallès, Spain). Calcium chloride (≥97%) was purchased from Honeywell International Inc. (Charlotte, NC, USA). Poly(ethylene glycol) (400) diacrylate (PEGDA, average M_n ≈ 520 g/mol), was purchased from IGM Resins (IGM resins, Gerenzano, Italy), Active Violet Ion (AVI) was provided by Procter & Gamble (Cincinnati, OH, USA), while Irgacure 1173 (2-hydroxy-2-methylpropiphenone, 97%) was supplied by Sigma Aldrich (Sigma Aldrich, Burlington, MA, USA). All the chemical compounds were used as provided without any further purification.

Preparation of the macrocapsules

The macrocapsules were synthesized following a reported procedure that involved different steps briefly detailed below[27]:

First of all, an aqueous solution of 500 mL containing 2% w/w $CaCl_2$ was prepared (crosslinking bath). Then, 200 mL of an aqueous polymeric solution consisting of a mixture of sodium alginate (1% w/w), the blue dye (0.8% w/w), PEGDA (1% w/w), and the photoinitiator (Irgacure 1173, 5% w/w PEGDA) was extruded over the calcium chloride crosslinking bath. The extrusion was done using a syringe-needle system located at 5.5 cm from the coagulation bath at a flowrate of 1 mL/min.

After that, the capsules were left 24 h stirring in the crosslinking bath (maturation step). The capsules that were prepared with PEGDA monomer were also irradiated at this phase during 5 min using an UV curing lamp from Helios Italquartz (50% power at 7.5 A). Two different irradiation times were chosen: directly after extrusion (Samples named A-PG-UV0h and A-PG-AVI0.8-UV0h) or after 24 h under magnetic stirring in the maturation bath (Samples labelled A-PG-UV24h and A-PG-AVI0.8-UV24h).

Finally, the collection step consisted of filtering and drying the capsules.

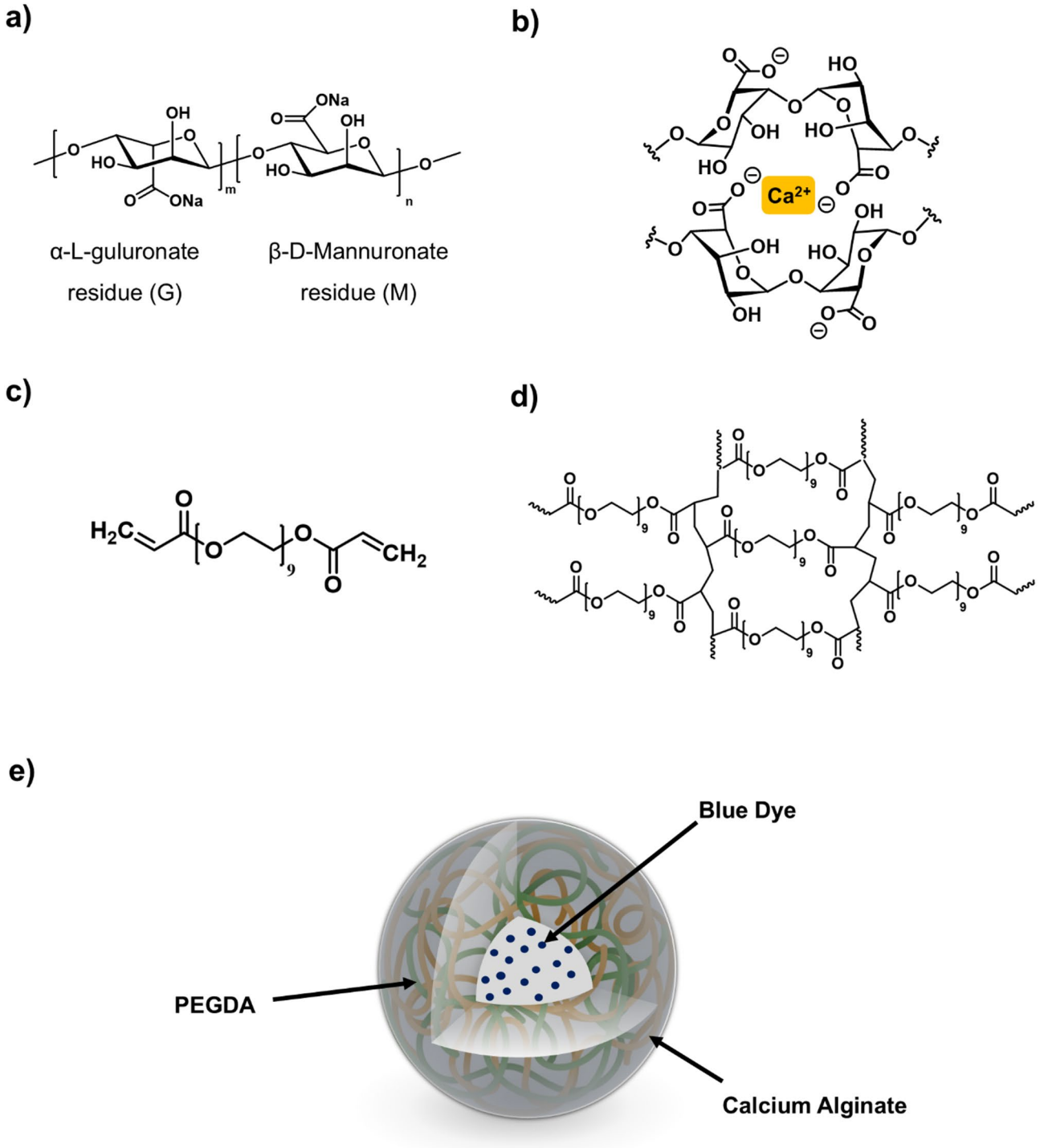

Fig. 1. Chemical structure of: (**a**) α-L-guluronate (G) and β-D-mannuronate (M) residues present in sodium alginate; (**b**) Crosslinking of alginate chains by calcium ions; (**c**) Poly (ethylene glycol) (400) diacrylate (PEGDA); (**d**) Crosslinked PEGDA; and e) general scheme of the synthesized capsules with the encapsulated blue dye.

The overall process followed is depicted in Fig. 2 and the chemical composition of each sample is summarized in Table 1.

Based on the composition and the pre-irradiation time selected for each system, the samples were labelled using specific acronyms: A for alginate, PG for PEGDA, and AVI0.8 for capsules loaded with 0.8% w/w dye. Moreover, UV0h and UV24h represent the time between the end of the extrusion and the UV irradiation during the samples stirring.

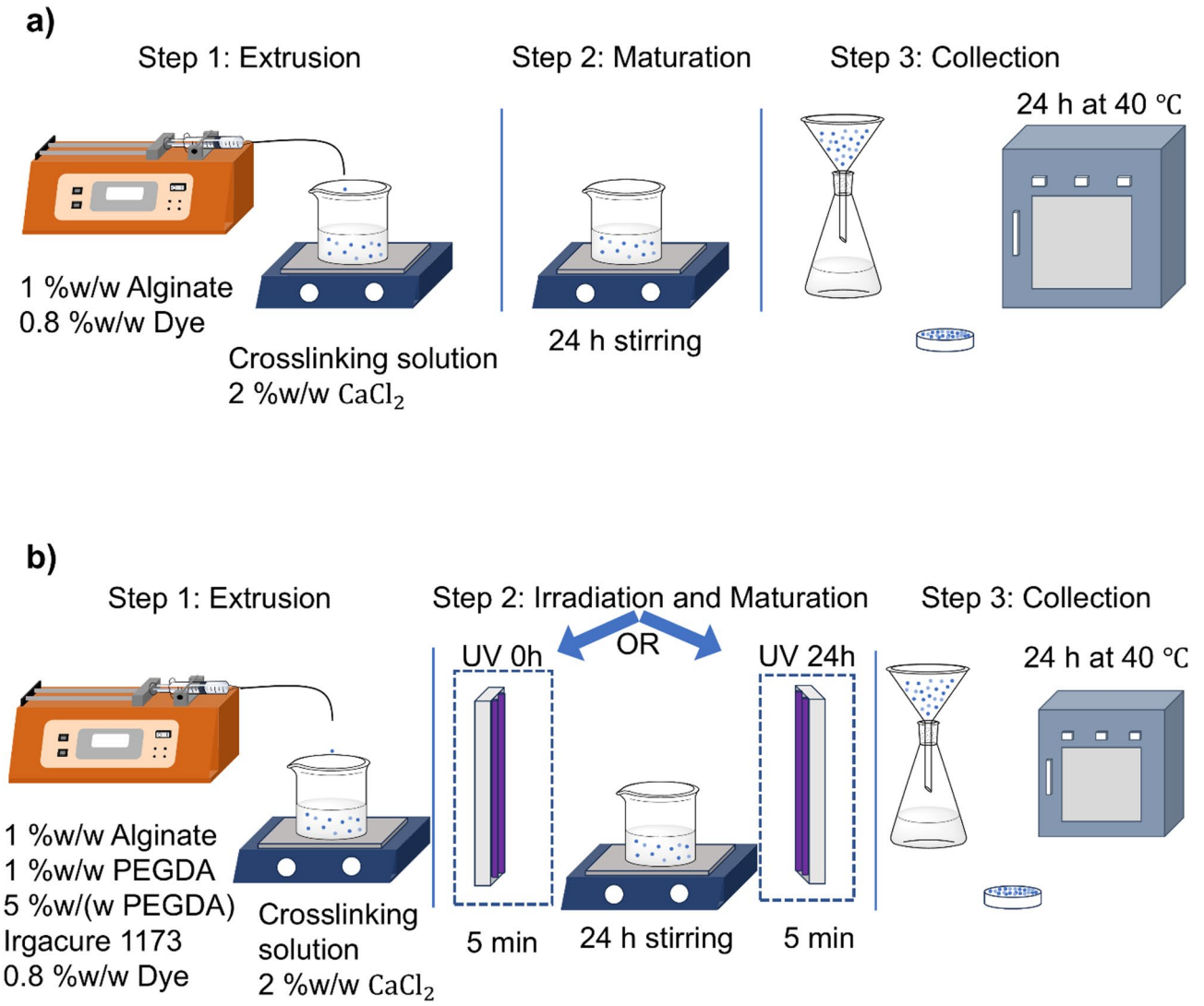

Fig. 2. Composition of the capsules and methodology followed in the dye encapsulation process of: (**a**) capsules which shell is only made of alginate; (**b**) Capsules which shell contains both alginate and PEGDA and were irradiated with UV light during 5 min before or after leaving them for 24 h under magnetic stirring.

Sample	Sodium alginate (% w/w respect to the polymeric solution)	PEGDA (% w/w respect to the polymeric solution)	Photoinitiator (Irgacure 1173) (% w/w respect to diacrylate monomer)	AVI (% w/w respect to the polymeric solution)	Time before UV irradiation (h) [a]
A	1	-	-	-	-
A-AVI0.8	1	-	-	0.8	-
A-PG-UV0h	1	1	5	-	0
A-PG-UV24h	1	1	5	-	24
A-PG-AVI0.8-UV0h	1	1	5	0.8	0
A-PG-AVI0.8-UV24h	1	1	5	0.8	24

Table 1. Composition of the prepared capsules. [a]At time = 0, the samples were irradiated just after the extrusion of the polymeric solution into the crosslinking solution, while at time = 24 h, the samples were irradiated after being stirred for 24 h together with the crosslinking solution.

Characterization

Fourier-transform infrared spectroscopy (FTIR)

The FTIR spectra of the samples were recorded on a Vertex 70 FTIR spectrophotometer from Bruker (Bruker Corporation, Billerica, MA, USA) in the wavelength range of 4000–300 cm^{-1} with an average of 16 scans and a resolution of 4 cm^{-1} in the absorbance mode. All the FTIR spectra were recorded at room temperature.

Elemental organic analysis

Elemental analysis was used to determine Carbon, Hydrogen and Nitrogen content of the following 2 samples: A-PG-UV0h and A-PG-UV24h (i.e., without any core material), by means of Perkin Elmer EA2400 Elemental Analyzer (Perkin Elmer, Waltham, MA, USA). Tests were performed in duplicate and the amount of analyzed capsules was approximately 3 mg.

Inductively coupled plasma optical emission spectrometry (ICP-OES)

Calcium and sodium contents in samples A-PG-UV0h and A-PG-UV24h were determined using an ICP-OES Agilent 5100 analyser (Agilent Technology, Santa Clara, CA, USA). The samples were analyzed in duplicate, after digestion overnight in HNO_3 or HCl. Around 2–3 mg of each sample were used for each analysis. Calcium and sodium concentrations were determined from the absorption intensities (Ca: 422.7 nm; Na: 589.6 nm) by interpolation of the calibration curves of intensity vs. concentration (ppm).

Optical microscopy (OM)

The prepared macrocapsules were observed with a Digital Microscope Leica DMS1000 (Wetzlar, Germany). The ImageJ (version 1.52, publicly available from the National Institutes of Health, Bethesda, MD, USA; http://imagej.nih.gov/ij/) software was used to measure the diameter of the capsules of each analyzed sample (The diameter of 20 capsules of each sample was measured before calculating the average value and its corresponding sampling error as shown in Table S1).

Environmental scanning electron microscopy (ESEM)

ESEM analysis were performed using a FEI Quanta 200 FEG (Hillsboro, OR, USA) in high vacuum mode, using a secondary electron detector and an accelerating voltage of 20 kV. Both the outer surface and the cross-section of the capsules were analyzed. Before the analysis, samples were coated on a tape surface with gold by means of a quorum Q150TS Plus sputter coater. To observe the cross-section, Leica CM 1950 Cryostat (Wetzlar, Germany) was used. The sample was mixed with an embedding medium (OCT Compound) and frozen at -25 ℃ on an aluminium support inside the machine. Once frozen, the sample was cut into slices of thickness 20 µm which were deposited on a microscopic slide.

Dynamic mechanical analysis (DMA)

Dynamic mechanical analysis was carried out using a DMA Q800 V21.3 Build 96 from TA instruments (New Castle, DE, USA) working on a controlled compression force on the capsule samples. 15 capsules from samples A-PG-AVI0.8-UV0h and A-PG-AVI0.8-UV24h were examined.

The temperature, the position of the probe, the force applied, the stress, the strain, the stiffness, the creep compliance and the relaxation modulus of each type of capsules were recorded with respect to the time until the rupture occurs under a ramp force of 2 N/min. The graph of the force versus displacement for each capsule was drawn to get the corresponding stress at break assuming that all capsules have a spherical shape. Furthermore, the Youngs modulus was calculated using Hertz theory and assuming a Poisson's ratio of 0.5[31,32].

Thermogravimetric analysis (TGA)

Thermal stability studies of the capsules were carried out in ALU OXIDE crucibles of 70 µL (ME-24123) with a Mettler Toledo TGA2 thermobalance (Mettler Toledo, Columbus, OH, USA). samples: A-PG-UV0h; A-PG-UV24h; A-PG-AVI0.8-UV0h and A-PG-AVI0.8-UV24h, weighing around 6–8 mg, were heated between 30 and 600 °C at a heating rate of 10 °C/min in N_2 atmosphere with a flow rate of 50 cm^3/min. The equipment was previously calibrated with indium (156.6 °C) and aluminium (660.3 °C) pearls.

Total organic carbon (TOC)

TOC is the amount of carbon found in an organic compound, which comes from oxidizing all organic matter present in water. It is commonly used to indicate the level of pollution in wastewater caused by organic compounds.

Basically, the TOC measurement is performed by converting all the kind of carbon from the sample into CO_2. There are direct and also indirect methods to carry out these measurements. The direct method was selected in our case.

In this method, the organic carbon (OC) was measured using the following steps:

- First of all, the inorganic carbon (IC) was removed through an acid treatment. Moreover, sample aeration prior to analysis eliminated errors due to the presence of inorganic carbon.
- In the second step, the OC content (or non-purgeable organic carbon (NPOC)) was determined by a chemical oxidation. The organic carbon of the sample was converted into CO_2 in a high temperature furnace. Finally, the CO_2 produced during the oxidation was measured by means of an FTIR detector.

In this way, TOC was quantitatively determined by interpolating the obtained values for each sample in the calibration curve prepared using potassium hydrogen phthalate (Sigma Aldrich, Burlington, MA, USA) as standard.

In this way, TOC analyses of the soluble fractions of samples A-PG-UV0h and A-PG-UV24h were carried out. To perform these analyses, first the water-soluble fraction of the capsules was obtained by this procedure: 500 mg of the capsules were crushed through a coffee grinding machine (MKM6003, BOSCH, Gerlingen, Germany) for 30 s. Then, the crushed samples were added to 50 mL of milliQ water and left under stirring for 24 h. At this time, the solution was filtered, and the remaining capsules were dried and weighed. The filtered solutions were analyzed using a Total Organic Carbon analyser TOC-L CSN 638-91109-48 equipment (Shimadzu Corporation, Kyoto, Japan). TOC analysis was repeated 3 times for each sample.

Results and discussion

Preparation of the macrocapsules

The control of the factors that could affect the polymerization to be able to encapsulate AVI in composite capsules constituted by alginate and poly(ethylene glycol) networks was already discussed in our recently published manuscript[27]. For these systems, the following criteria had been established:

- Active Violet Ion (AVI) was chosen as a dye due to its stability inside the capsules.
- The optimal dye concentration in the formulations was set at 0.8% respect to the polymeric water solution since this concentration corresponds to the maximum solubility of the dye in water.

Summing up, new composite capsules with high molecular weight PEGDA and alginate have been synthesized using the previously reported procedure[27].

Characterization of the macrocapsules

The synthesized capsules, which shell is constituted by alginate and a poly(ethylene glycol) network derived from crosslinking PEGDA, were characterized using different techniques. In this research work, our studies focused on:

- The determination of the effect of the chemical structure of the starting diacrylate monomer (PEGDA or PEGDMA) employed together with alginate to form the biobased composite shell in the final properties of the obtained capsules.
- The impact of the conditions used during capsule preparation on the final properties they exhibit when they were prepared with PEGDA monomer.

Chemical characterization

The chemical composition of the new capsules was determined by Fourier-transform infrared spectroscopy (FTIR), elemental organic analysis and inductively coupled plasma optical emission spectroscopy (ICP-OES).

Figure 3 shows the FTIR spectra of PEGDA diacrylate monomer, sodium alginate and samples A, A-PG-UV0h and A-PG-UV24h. The comparison of the spectra of both monomers alone before crosslinking (PEGDA and sodium alginate) with the composite capsules exhibit evidences that both crosslinking reactions involving each of the two monomers introduced into the formulations (ionic gelation of alginate and radical polymerization of PEGDA) took place, forming the shell of the capsules[27]: as observed in the FTIR spectrum of sodium alginate, the broad band associated to the ν(O-H) stretching (3245 cm^{-1}) and the band attributed to the asymmetric ν(COO^-) stretching (1404 cm^{-1}) are shifted to higher wavenumbers (around 3360 cm^{-1} and 1430 cm^{-1}, respectively) when the crosslinking of alginate occurred, as can be seen in the FTIR spectra of samples A-PG-UV0h and A-PG-UV24h, respectively[33,34]. Additionally, the ν(O-H) stretching band narrows and presents a higher intensity due to the greater quantity of intramolecular hydrogen bonds in the crosslinked alginate[35]. Besides, the lower intensity of the band attributed to the ν(C-O-C) stretching (around 1026 cm^{-1}) in the polymerized samples also confirms that alginate gelation occurred[36].

On the other hand, the intensity drops of the characteristic bands of the diacrylate monomer attributed to the δ(C=C) bending (951 cm^{-1}) and δ(C=C) twisting (810 cm^{-1}), respectively, corroborates that PEGDA polymerization took place during the UV irradiation of formulations A-PG-UV0h and A-PG-UV24h[37–40]. Preliminary investigations allowed us to determine that these systems needed to be irradiated with UV light for 5 min to achieve complete crosslinking of the diacrylate monomer[27]. Furthermore, the observation of the bands attributed to the ν(C=O) stretching of diacrylate groups that appear in the spectra of these 2 samples (1732 cm^{-1} for A-PG-UV0h and 1728 cm^{-1} for A-PG-UV24h) also confirms that polymerized PEGDA is part of the final network[41]. As we had verified with the capsules reported in our previous work, the incorporation of the dye inside the capsules does not produce any substantial difference in the FTIR spectra of the capsules with and without the encapsulated AVI dye since recorded spectra were practically identical (Figure S1). This information corroborates that the dye had been effectively encapsulated[42].

Table 2 reports the results of the elemental analysis and ICP-OES of the investigated capsules. These results were practically identical to those obtained for the capsules containing alginate and PEGDMA monomer[27]. Nevertheless, they differ in the amount of calcium, which is lower in the samples prepared with PEGDA and alginate (around 10.8% by weight in the composite capsules prepared with PEGDA, compared to 12.2% in the composite capsules prepared with PEGDMA), which confirms our previous hypothesis that the addition of PEGDA monomer could reduce the gelation capacity of Ca^{2+}[43].

[a] Only one sample could be analyzed by ICP-OES.

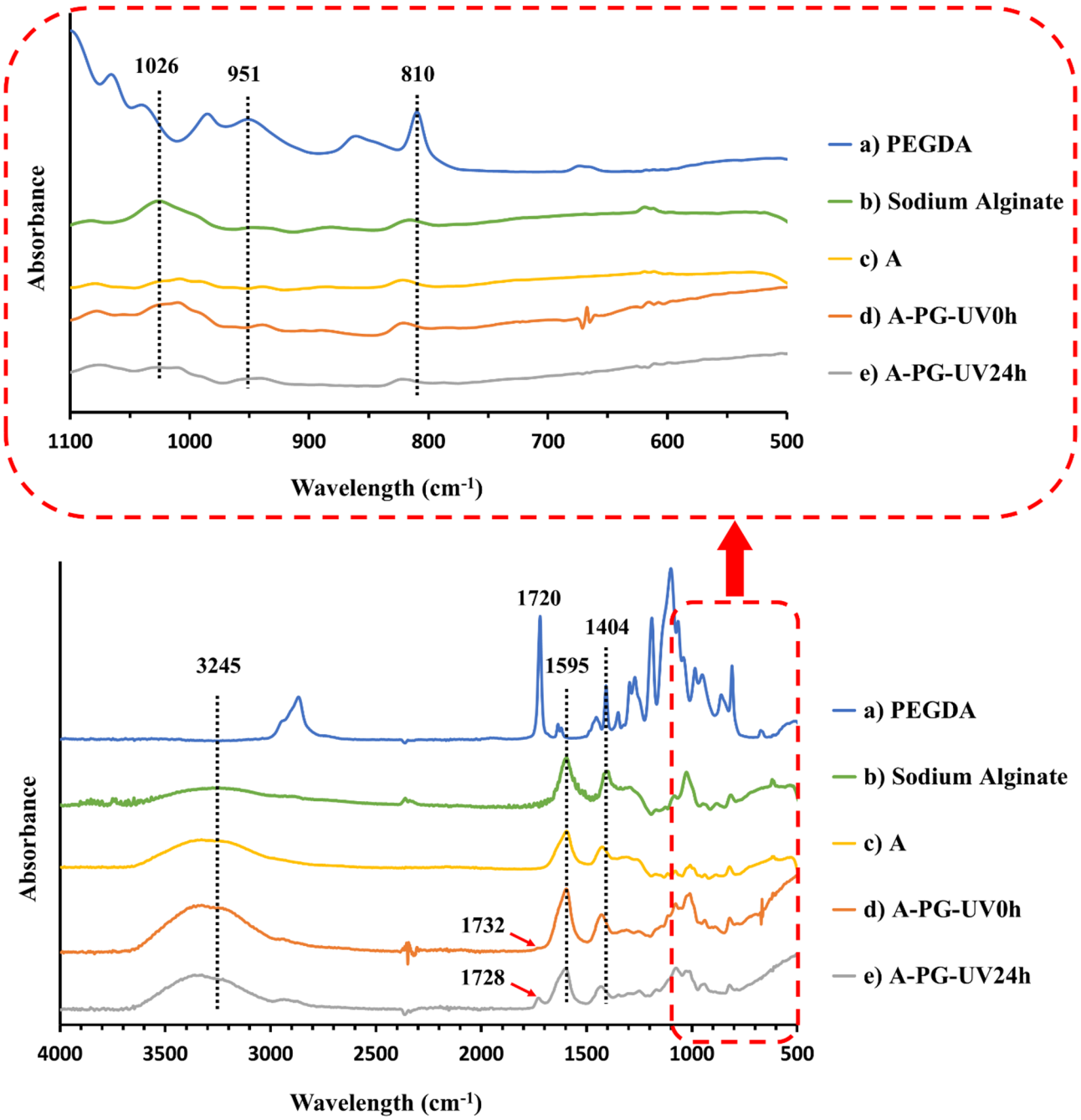

Fig. 3. FTIR spectra of: a) PEGDA; b) Sodium alginate; c) A; d) A-PG-UV0h; and e) A-PG-UV24h.

Sample	Weight (%)				
	C	H	*N*	Ca	Na
A-PG-UV0h	18.4 ± 0.2	4.46 ± 0.04	0.30 [a]	10.7 ± 0.1	0.39 ± 0.01
A-PG-UV24h	18.6 ± 0.2	4.52 ± 0.07	0.30 [a]	10.8 ± 0.4	0.39 ± 0.01

Table 2. Elemental composition determined by elemental organic analysis and ICP-OES (%).

Morphological characterization

The morphology of these macrocapsules was characterized by optical microscopy (OM) and environmental scanning electron microscopy (ESEM). As observed in Fig. 4a, the capsules of all the samples present a uniform and round structure. Moreover, neither the incorporation of PEGDA monomer in the shell of the capsule nor

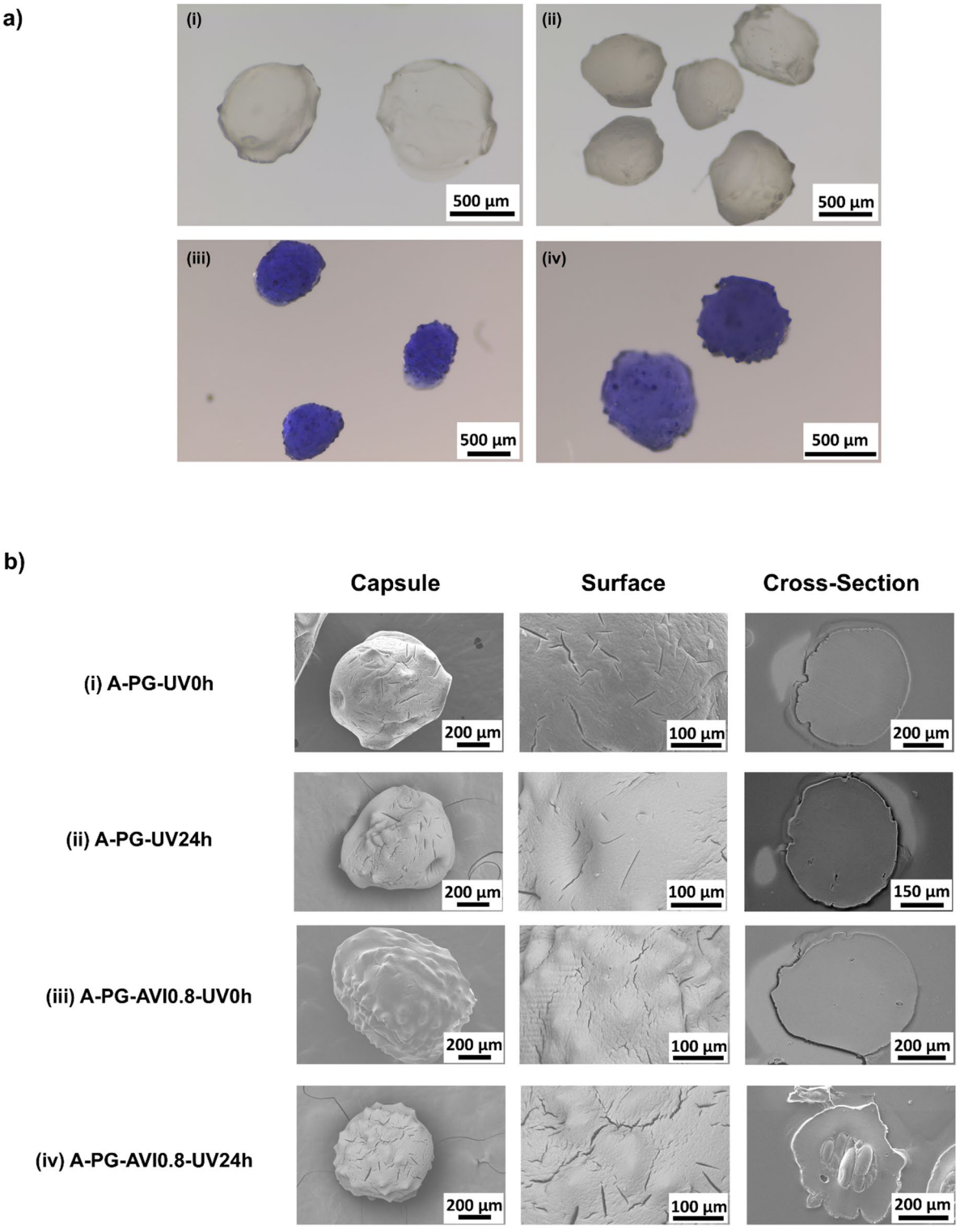

Fig. 4. (**a**) Optical microscope images of capsules of the following samples: (i) A-PG-UV0h, (ii) A-PG-UV24h, (iii) A-PG-AVI0.8-UV0h and (iv) A-PG-AVI0.8-UV24h; (**b**) ESEM images of synthesized capsules showing the whole capsule (magnification x160), its surface (magnification x500) and its cross-section (magnification x200, x285, x235, and x245 for A-PG-UV0h, A-PG-UV24h, A-PG-AVI0.8-UV0h and A-PG-AVI0.8-UV24h, respectively): (i) A-PG-UV0h, (ii)A-PG-UV24h, (iii) A-PG-AVI0.8-UV0h and (iv) A-PG-AVI0.8-UV24h.

the encapsulation of the blue dye affected the shape or size of the capsules, which had average diameters between 0.62 and 0.71 mm (Table S1)[44,45]. In this case, the size of the capsules is only determined by the diameter of the syringe needle used during the extrusion of the polymeric solution in the crosslinking bath[46]. Furthermore, the particle size distribution of the samples showed that the capsules irradiated after 24 h present a slightly narrower size distribution (Figure S2).

On the other hand, the encapsulation of the dye affects the morphology of the capsules, as shown in Fig. 4b. Samples A-PG-AVI0.8-UV0h and A-PG-AVI0.8-UV24h, which capsules contain the encapsulated blue dye, exhibited a rougher surface than empty capsules since the interactions between the dye and alginate hinders its crosslinking process[47,48].

Another parameter whose effect was studied is the irradiation time of the capsules since the capsules of sample A-PG-AVI0.8-UV0h were irradiated directly after the extrusion process, while the capsules of sample A-PG-AVI0.8-UV24h were irradiated after being for 24 h in the crosslinking solution. The largest number of cracks present on the surface of the capsules of sample A-PG-AVI0.8-UV24h together with the hollow spheres detected in their cross-section confirmed that these capsules present a more heterogeneous structure compared to capsules of sample A-PG-AVI0.8-UV0h. The choice of irradiation time explains the formation of a more irregular capsule shell. In this case, the photopolymerization of the diacrylic monomer (PEGDA) is not favoured until 24 h after preparing the mixture. At this time, alginate crosslinking is expected to have already taken place and that the remaining gaps in the shell of the capsules will be filled by the polymerized PEGDA once the formulation was irradiated with the UV lamp. In the sample which was irradiated directly after extrusion, the polymerization of PEGDA was initiated directly at the same time that alginate starts to gel, resulting in the formation of a more homogeneous structure.

Previous investigations by our research group proved that most of the maturation processes involving alginate gels were complete after 24 h[49]. The morphology of the capsules prepared in this work, which involves an alginate-PEGDA interpenetrating network, is affected by two key factors: maturation time and UV irradiation. To evaluate the relative impact of these factors, ESEM images were taken during the preparation of the different samples to analyse how each factor influences the morphology (Fig. 5a). For the alginate capsules, comparing sample A (t = 0 h) with the image taken after 24 h of maturation presented in our previous work[27], it was shown that the surface smoothness increases with maturation. A similar increase in smoothness was also observed after irradiating sample A-PG-UV0h with UV light, as seen when comparing the images taken before (t = 0 h, before irradiation) and after irradiation (t = 0 h, after irradiation). Therefore, UV irradiation affects surface morphology to some extent. However, this effect was not evident when comparing the image of sample A-PG-UV24h (t = 24 h, before irradiation) with the images shown in Fig. 4b-ii. These images depict sample A-PG-UV24h after 24 h of maturation, both before and after UV irradiation, respectively, and there was no significant difference between their morphology. In contrast, comparing the images of sample A-PG-UV0h (t = 0 h, before irradiation) and A-PG-UV24h (t = 24 h, before irradiation), again showed that the surface smoothness increased when the capsules were left to mature for 24 h. This suggests that maturation time is the predominant factor influencing the capsules morphology. Additionally, Fig. 5b shows that the capsules' diameter decreased both after UV irradiation and after maturation, which was expected due to syneresis.

Regarding the diacrylic monomer used in the preparation of the capsules, the empty capsules which shell is constituted by a mixture of polymerized PEGDA and alginate showed greater homogeneity compared to the capsules prepared using PEGDMA and alginate[27]. This fact could be attributed to the expected greater reactivity of PEGDA acrylate groups compared to PEGDMA methacrylate groups, which confirmed our hypothesis and leads to the formation of a more regular networks when PEGDA was used[50]. When the capsules with the encapsulated blue dye were compared, those that were prepared with PEGDA and that were irradiated after 24 h showed a more heterogeneous structure in contrast to those prepared with PEGDMA and irradiated after 24 h[27]. This greater heterogeneity can be explained by two factors: firstly, the intermolecular interactions that take place between AVI dye, calcium and the growing crosslinked network. Secondly, the difference in the reactivity of the diacrylic monomers may also explain these remarkable differences in morphology since PEGDA can begin to polymerize even before being irradiated by UV light during the gelation of alginate, which would explain that sample A-PG-AVI0.8-UV24h present the less uniform crosslinked network[51]. On the other hand, for the capsules irradiated directly after extrusion, the ones with PEGDA were more homogeneous while the ones with PEGDMA presented a more heterogeneous cross-section. This can be attributed to the lower reactivity of the methacrylate groups of PEGDMA due to the steric hindrance of the methyl groups adjacent to the double bond that hinder the polymerization of this monomer compared to PEGDA. Moreover, when the irradiation of PEGDMA finishes, the methacrylate groups still present in the crosslinked network can act as a barrier for the penetration of calcium and the dye inside the capsule during the maturation phase.

Mechanical characterization

The mechanical properties of the samples A-PG-AVI0.8-UV0h and A-PG-AVI0.8-UV24h were studied using DMA (Table 3). The values of Young's modulus and the stress at break of these samples were compared under continuous compression tests. As expected, the capsules containing PEGDA resulted mechanically stronger, as they exhibited a higher Young's modulus than the capsules prepared only with alginate, which indicates that the composite networks are more crosslinked in the presence of PEGDA (Table 3 and S2). This is in agreement with the literature, since different studies report that mechanical properties are enhanced in the presence of a densely crosslinked interpenetrating network. For example, Mamaghani et al. showed that increasing the concentration of polymers in the interpenetrating network based on gelatin methacrylate/PEGDA/graphine oxide enhanced crosslinking and, consequently, improved the mechanical properties[52]. Moreover, Jin et al. proved that composite zirconia scaffolds with an interpenetrating network of alginate and gelatin methacrylate exhibited a higher compressive modulus compared to bare zirconia scaffolds[53]. Additionally, a comparison of these capsules with

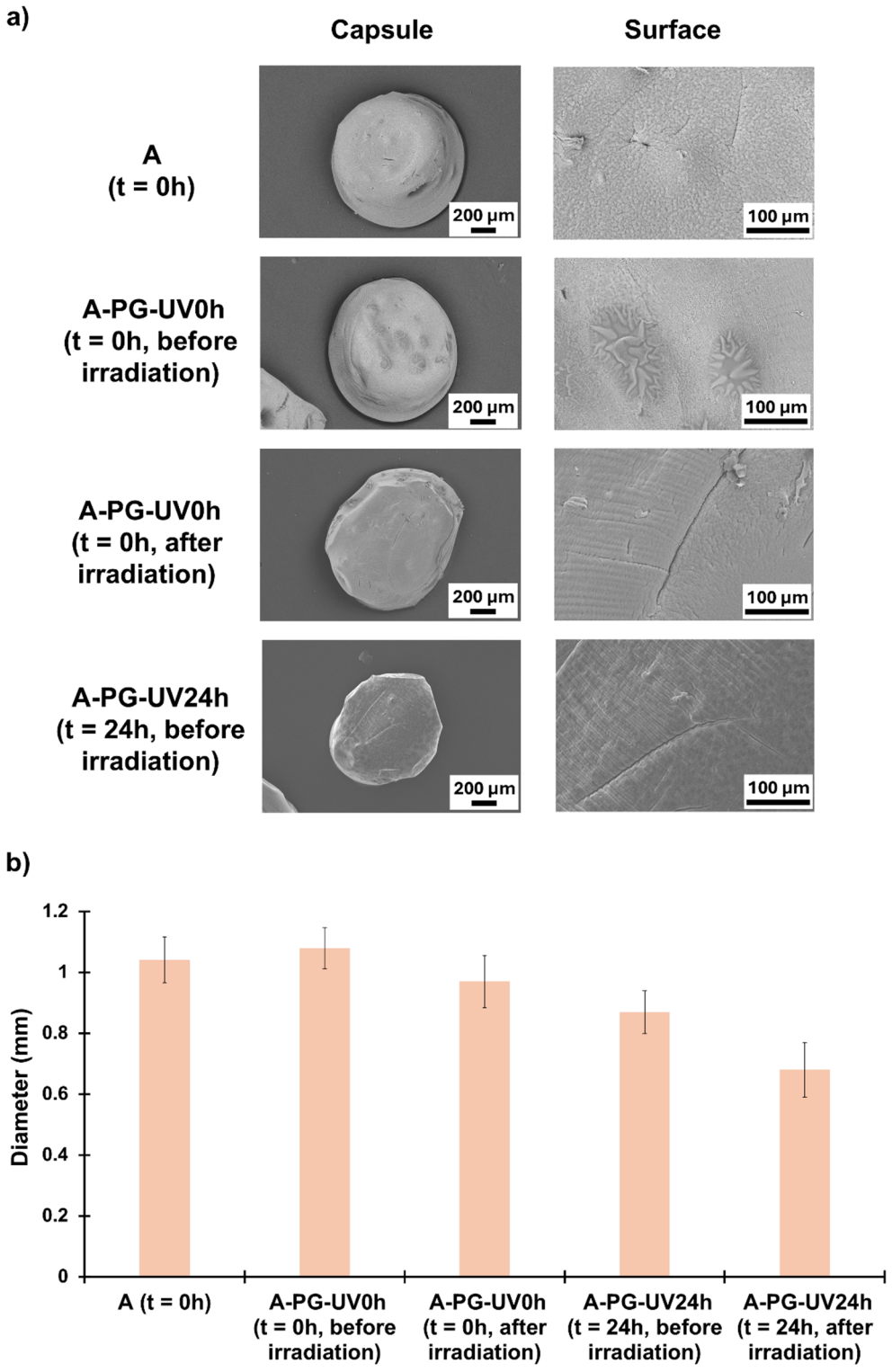

Fig. 5. (**a**) ESEM images of the capsules (magnification x100) and their surface during their preparation (magnification x500); and (**b**) Diameters of the different types of capsules investigated during their preparation.

those previously prepared using PEGDMA (Table S2) showed a significant increase in the Young's modulus in capsules containing PEGDA (Table 3), which can be attributed to a more compact and mechanically stronger structures[54].

Comparing the samples A-PG-AVI0.8-UV0h and A-PG-AVI0.8-UV24h, it was shown that the capsules containing the dye and that were irradiated directly after extrusion had a more rigid structure giving higher values of the stress at break and Young's modulus compared to the capsules irradiated after 24 h (Table 3). The

Sample	Young's Modulus (E, MPa)	Stress at break σb (MPa)
A-PG-AVI0.8-UV0h	1587 ± 438	22.5 ± 5.2
A-PG-AVI0.8-UV24h	1171 ± 391	16.9 ± 3.4

Table 3. Young's modulus and the stress at break of the capsules.

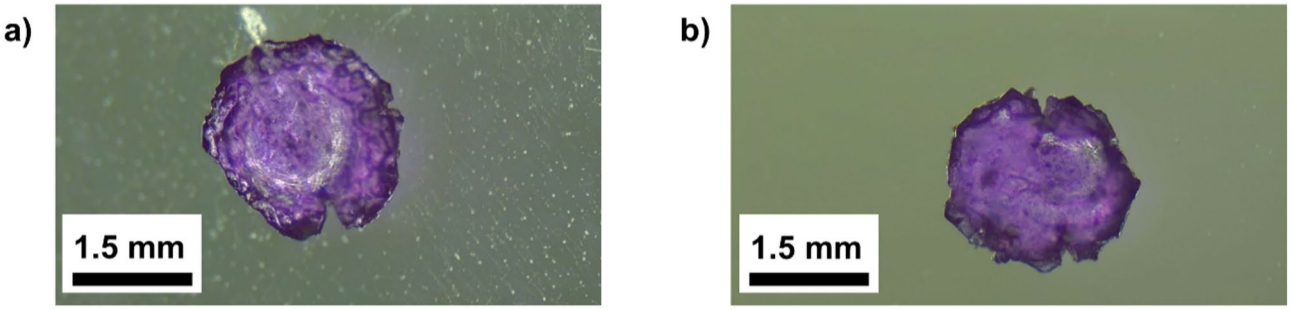

Fig. 6. Optical microscope images of samples after compression tests of: (**a**) A-PG-AVI0.8-UV0h and (**b**) A-PG-AVI0.8-UV24h.

Sample	$T_{5\%}$ (°C) [a]	Char yield (%) [b]
A-PG-UV0h	137	46.8
A-PG-UV24h	129	45.7
A-PG-AVI0.8-UV0h	140	44.3
A-PG-AVI0.8-UV24h	142	45.3

Table 4. The onset temperature of 5% weight loss and the remaining Char yield (%) of the investigated samples. [a]Temperature of 5% weight loss. [b]Char residue at 600 °C.

more regular and homogeneous structure of the capsules from sample A-PG-AVI0.8-UV0h compared to sample A-PG-AVI0.8-UV24h, which was proved by OM and ESEM (Fig. 4), confirmed that the capsules irradiated at time 0 h have a more compact and rigid structure.

On the other hand, the three types of capsules investigated reacted in an elastoplastic way to the compression force and after the compression test the capsules were flattened and had small cracks in their structure (Fig. 6). However, complete fracture of the capsules was not observed[49]. In this way, it is expected that these new composite capsules will present greater stability during their processing and the time they will remain stored until their use is required in the washing of fabrics.

Thermal characterization

The thermal stability of the following samples: A-PG-UV0h, A-PG-UV24h, A-PG-AVI0.8-UV0h, and A-PG-AVI0.8-UV24h was examined using thermogravimetric analysis (TGA) and the obtained results were compared with those reported in our previous work[27]. TGA and DTGA curves are shown in Figures S3 and S4. The thermal decomposition onset, reported as $T_{5\%}$, and the char yield, are depicted in Table 4.

The thermal degradation of the capsules occurs in four steps. The first degradation step which is attributed to the loss of water occurs between 43 and 180 °C. The percentage of water in these capsules, which was 9%, was lower compared to that in the alginate-based capsules (14%), and in the previously reported capsules based on PEGDMA-alginate (16%). This step is followed by the second and third steps, which correspond to the degradation of crosslinked alginate[27,55]. The last degradation step, which is located between 363 and 446 °C, is assigned to the degradation of PEGDA network[56,57]. As shown in TGA and DTGA curves, the different irradiation times selected and the presence of the dye do not affect the thermal degradation of these capsules.

Furthermore, the onset of thermal weight loss (determined as the temperature corresponding to 5% mass loss) was calculated for all the studied samples (Table 4). When we compared the capsules prepared with PEGDA, the lowest $T_{5\%}$ was presented by the capsules without the encapsulated AVI dye that were irradiated after 24 h: 129 ℃, while the same capsules but with the encapsulated dye presented the highest $T_{5\%}$ value: 142 ℃. All the capsules irradiated just after the extrusion, both with and without dye, presented values similar to this last value. However, these values are higher than those presented by the capsules synthesized using only alginate, showing that the addition of PEGDA increased their thermal stability. In any case, there was no significant variation in the values of the remaining char yield at 600 °C for the different samples, which was around 45%.

Sample	Mass fraction of the capsules dissolved (wt%) [a]	TOC (mg/L)
A-PG-UV0h	52 ± 4	287 ± 2
A-PG-UV24h	49 ± 1	300 ± 7

Table 5. The mass fraction of the capsules dissolved in water (wt%) and TOC results of the investigated samples. [a]After 1 day in water.

On the other hand, the substitution of PEGDMA by PEGDA monomer also produced an improvement in the thermal stability of the capsules as can be seen by comparing the values of the onset temperature for the 5% weight loss. Indeed, $T_{5\%}$ of the PEGDA-based systems are around 30 °C higher for the capsules without the encapsulated dye and around 55 °C higher for the samples containing the encapsulated dye[27]. This greater thermal stability may be due to the higher degree of crosslinking of PEGDA compared to PEGDMA caused by the steric hindrances of the dimethacrylate monomer, which hinder the homopolymerization of PEGDMA.

Water solubility studies of the capsules

The water solubility of the samples and the total organic carbon of the water-soluble fractions of the capsules were determined. Table 5 shows the percentage of the dissolved mass fraction and the TOC values of the studied samples. It was demonstrated that the water solubility of the capsules was slightly affected by the addition of PEGDA in the network comparing them to the alginate-based capsules reported before[27]. For the sample A-PG-UV0h, the mass fraction dissolved was equal to 52.2% while it was a little bit lower in the case of sample A-PG-UV24h: 48.9% Both values are slightly higher than the solubility of alginate-based capsules: 45.6% In this way, the presence of PEGDA in the capsules reduced the gelation capacity of alginate, as previously demonstrated, and this made them slightly more soluble[58].

The TOC resulting from the soluble fractions of the alginate capsules showed the lowest value, which is equal to 30.5 ± 8.5 mg/L, while this value increases around 10 times for the capsules that contained PEGDA (around 300 mg/mL). Although the dissolved mass fraction of these different samples was similar, there was a large difference in the TOC values when PEGDA was incorporated into the formulations. Furthermore, these values of TOC are very similar than the ones measured for the capsules prepared using PEGDMA and alginate[27]. Besides, there are no significant differences between the composite capsules made of PEGDA and alginate and those prepared with PEGDMA and alginate in terms of their TOC content and water solubility. In both cases, the capsules irradiated with UV light directly after extrusion were slightly more soluble than the capsules irradiated after 24 h. This could be related to the fact that the irradiation of these capsules, which leads to the chemical crosslinking of the diacrylate monomers directly after extrusion, decreases the gelation capacity of alginate and gives rise to more soluble composite capsules. However, the ones irradiated after 24 h have enough maturation time for the alginate to effectively crosslink, thus forming the shell of the capsules before they were irradiated with UV light.

Conclusions

Biobased capsules constructed from an interpenetrating network of alginate and PEGDA ($M_n \approx 520$ g/mol) were prepared. Moreover, the AVI dye was successfully encapsulated in these capsules. Changing the composition and the time at which the capsules were irradiated allowed the formation of capsules with different chemical, morphological, thermal, and mechanical properties. The introduction of PEGDA instead of PEGDMA was expected to improve mechanical properties and thermal stability of the final interpenetrated network, based on higher reactivity of acrylate versus methacrylate groups.

The crosslinking of both monomers was confirmed by monitoring their characteristic bands in the FTIR spectra for all the capsules. As regards their form, all the capsules showed a spherical shape. Nevertheless, they differ in their morphology: the capsules which were irradiated directly after extrusion showed a homogeneous and compact structure, while the capsules irradiated after 24 h exhibited a more heterogeneous morphology probably because after 24 h the alginate chains were already crosslinked and the subsequent PEGDA crosslinking would be restricted by the alginate network. The incorporation of the AVI dye inside the capsules also increased the roughness of its surface.

Concerning their mechanical properties, the composite capsules prepared with PEGDA and alginate showed a higher Young's modulus and stress at break compared to both the alginate capsules and the composite capsules prepared with alginate and PEGDMA, which was expected due to the higher number of crosslinking points. All the capsules showed an elastoplastic behavior upon compression. Moreover, the substitution of PEGDMA monomer by PEGDA in the formulations provided greater thermal stability to these novel composite capsules that can endure temperatures around 130–140 °C.

In conclusion, the composite capsules constituted by alginate and poly(ethylene glycol) network derived from PEGDA monomer demonstrated notable satisfactory mechanical strength and thermal stability, positioning these capsules as highly promising candidates for applications in laundry detergents.

Data availability

All data generated or analysed during this study are included in this published article [and its supplementary information files].

Received: 26 November 2024; Accepted: 2 June 2025
Published online: 01 July 2025

References

1. Aguiar, A. et al. Microcapsules of Poly(butylene adipate-co-terephthalate) (PBAT) Loaded with Aliphatic Isocyanates for Adhesive Applications. *ACS Appl. Polym. Mater.* **6**, 5618–5629 (2024).
2. Aguiar, A., Loureiro, M. V., Pinho, I. & Marques, A. C. Efficient encapsulation of isocyanates in PCL/PLA biodegradable microcapsules for adhesives. *J. Mater. Sci.* **58**, 2249–2267 (2023).
3. Machado, T. O. et al. Biopolymer-based nanocarriers for sustained release of agrochemicals: A review on materials and social science perspectives for a sustainable future of agri- and horticulture. *Adv. Colloid Interface Sci.* **303**, 102645 (2022).
4. Radulescu, D. M., Neacsu, I. A., Grumezescu, A. M. & Andronescu, E. New insights of scaffolds based on hydrogels in tissue engineering. *Polym. (Basel).* **14**, 799 (2022).
5. Tomadoni, B., Fabra, M. J. & López-Rubio, A. Electrohydrodynamic processing of phycocolloids for food-related applications: recent advances and future prospects. *Trends Food Sci. Technol.* **125**, 114–125 (2022).
6. Shoeibi, S. et al. Recent advancements in applications of encapsulated phase change materials for solar energy systems: A state of the Art review. *J. Energy Storage*. **94**, 112401 (2024).
7. Sousa, V. I., Parente, J. F., Marques, J. F., Forte, M. A. & Tavares, C. J. Microencapsulation of essential oils: A review. *Polym. (Basel).* **14**, 1730 (2022).
8. Jiao, M., Zhang, Y., Dong, Z., Zhang, H. & Jiang, Y. Microencapsulation of multi-component traditional Chinese herbs extracts and its application to traditional Chinese medicines loaded textiles. *Colloids Surf. B Biointerfaces*. **240**, 113970 (2024).
9. Kumar, D., Gautam, A., Rohatgi, S. & Kundu, P. P. Synthesis of vildagliptin loaded acrylamide-g-psyllium/alginate-based core-shell nanoparticles for diabetes treatment. *Int. J. Biol. Macromol.* **218**, 82–93 (2022).
10. Hedayati, S., Tarahi, M., Iraji, A. & Hashempur, M. H. Recent developments in the encapsulation of lavender essential oil. *Adv. Colloid Interface Sci.* **331**, 103229 (2024).
11. Saberi Riseh, R., Vatankhah, M., Hassanisaadi, M. & Kennedy, J. F. Macromolecules-based encapsulation of pesticides with carriers: A promising approach for safe and effective delivery. *Int. J. Biol. Macromol.* **269**, 132079 (2024).
12. Manga, M. S. et al. Deposition and retention of differently shaped micro-particles on textiles during laundry processing. *Powder Technol.* **398**, 117143 (2022).
13. Bojana, B. P. & Marica, S. Microencapsulation technology and applications in added-value functional textiles. *Phys. Sci. Reviews*. **1**, 20150003 (2019).
14. Polaris Market Research. *Laundry Detergent Market Share, Size, Trends, Industry Analysis Report, By Product (Natural/Eco-Friendly Detergents, Powder, Liquid, Fabric Softeners, Detergent Tablets, Washing Pods); By Application (Household, Industrial); By Region; Segment Forecast, 2*. (2021). https://www.marketresearch.com/Polaris-Market-Research-Consulting-LLP-v4237/Laundry-Detergent-Share-Size-Trends-30881720/
15. Smulders, E., Sung, E. & Laundry Detergents 2. Ingredients and Products. in *Ullmann's Encyclopedia of Industrial Chemistry* vol. 20 393–447 (Wiley-VCH, (2012).
16. He, Y. et al. Synthesis of melamine-formaldehyde microcapsules containing oil-based fragrances via intermediate polyacrylate bridging layers. *Chin. J. Chem. Eng.* **27**, 2574–2580 (2019).
17. Mamusa, M., Resta, C., Sofroniou, C. & Baglioni, P. Encapsulation of volatile compounds in liquid media: fragrances, flavors, and essential oils in commercial formulations. *Adv. Colloid Interface Sci.* **298**, 102544 (2021).
18. Soltanpour, Z., Mohammadian, Y. & Fakhri, Y. The exposure to formaldehyde in industries and health care centers: A systematic review and probabilistic health risk assessment. *Environ. Res.* **204**, 112094 (2022).
19. Rana, I., Rieswijk, L., Steinmaus, C. & Zhang, L. Formaldehyde and brain disorders: A Meta-Analysis and bioinformatics approach. *Neurotox. Res.* **39**, 924–948 (2021).
20. De-la-Torre, G. E. Microplastics: an emerging threat to food security and human health. *J. Food Sci. Technol.* **57**, 1601–1608 (2020).
21. Charlton-Howard, H. S., Bond, A. L., Rivers-Auty, J. & Lavers, J. L. 'Plasticosis': Characterising macro- and microplastic-associated fibrosis in seabird tissues. *J Hazard Mater* 450, 131090 (2023).
22. Rotchell, J. M. et al. Detection of microplastics in human saphenous vein tissue using μFTIR: A pilot study. *PLoS One* **18**, (2023).
23. Directorate-General for Internal Market. Industry & Entrepreneurship and SMEs. REACH committee votes to restrict intentional microplastics. (2023). https://single-market-economy.ec.europa.eu/news/reach-committee-votes-restrict-intentional-microplastics-2023-04-27_en
24. Reig-Vano, B., Tylkowski, B., Montané, X. & Giamberini, M. Alginate-based hydrogels for cancer therapy and research. *Int. J. Biol. Macromol.* **170**, 424–436 (2021).
25. Ramos, R., Bernard, J., Ganachaud, F. & Miserez, A. Protein-Based encapsulation strategies: Toward Micro- and nanoscale carriers with increased functionality. *Small Sci.* **2**, 2100095 (2022).
26. Wang, Y. et al. Chitosan cross-linked poly(acrylic acid) hydrogels: Drug release control and mechanism. *Colloids Surf. B Biointerfaces*. **152**, 252–259 (2017).
27. Kabalan, Y., Montané, X., Tylkowski, B., De la Flor, S. & Giamberini, M. Design and assembly of biodegradable capsules based on alginate hydrogel composite for the encapsulation of blue dye. *Int. J. Biol. Macromol.* **233**, 123530 (2023).
28. Pérez-Mondragón, A. A., Cuevas-Suárez, C. E., González-López, J. A., Trejo-Carbajal, N., & Herrera-González, A. M. Evaluation of new coinitiators of camphorquinone useful in the radical photopolymerization of dental monomers. *J. Photochem. Photobiol Chem.* **403**, 112844 (2020).
29. Nam, C., Yoon, J., Ryu, S. A., Choi, C. H. & Lee, H. Water and oil insoluble PEGDA-Based microcapsule: Biocompatible and multicomponent encapsulation. *ACS Appl. Mater. Interfaces*. **10**, 40366–40371 (2018).
30. Ahn, S. H., Rath, M., Tsao, C. Y., Bentley, W. E. & Raghavan, S. R. Single-Step synthesis of alginate microgels enveloped with a covalent polymeric shell: A simple way to protect encapsulated cells. *ACS Appl. Mater. Interfaces*. **13**, 18432–18442 (2021).
31. Chan, E. S. et al. Effect of formulation of alginate beads on their mechanical behavior and stiffness. *Particuology* **9**, 228–234 (2011).
32. Kaygusuz, H., Evingür, G. A., Pekcan, Ö., von Klitzing, R. & Erim, F. B. Surfactant and metal ion effects on the mechanical properties of alginate hydrogels. *Int. J. Biol. Macromol.* **92**, 220–224 (2016).
33. Chen, N., Feng, Z. J., Gao, H. X., He, Q. & Zeng, W. C. Core-shell structured alginate-based hydrogel beads modified by starch and Protocatechuic acid: preparation, characterization, phenolic slow release and stable antioxidant potential. *Food Chem.* **459**, 140389 (2024).
34. Dash, S., Gutti, P., Behera, B. & Mishra, D. Anionic species from multivalent metal salts are differentially retained during aqueous ionic gelation of sodium alginate and could fine-tune the hydrogel properties. *Int. J. Biol. Macromol.* **265**, 130767 (2024).
35. Castro, R. I. et al. Design and optimization of a self-assembling complex based on microencapsulated calcium alginate and glutathione (Cag) using response surface methodology. *Polym. (Basel).* **13**, 2080 (2021).
36. Kusuktham, B., Prasertgul, J. & Srinun, P. Morphology and property of calcium silicate encapsulated with alginate beads. *Silicon* **6**, 191–197 (2014).
37. Deutsch Lukatsky, A. T., Dan, Y., Mizrahi, L. & Amir, E. Hydrogels based on crosslinked polyethylene glycol diacrylate and fish skin gelatin. *Eur. Polym. J.* **210**, 112990 (2024).

38. Hemmatgir, F., Koupaei, N. & Poorazizi, E. Characterization of a novel semi-interpenetrating hydrogel network fabricated by polyethylene glycol diacrylate/polyvinyl alcohol/tragacanth gum as a wound dressing. *Burns* **48**, 146–155 (2022).
39. Magalhães, L. S. S. M. et al. Nanocomposite hydrogel produced from PEGDA and laponite for bone regeneration. *J. Funct. Biomater.* **13**, 53 (2022).
40. Miranda, B., Dello Iacono, S., Rea, I., Borbone, F. & De Stefano, L. Effect of the molecular weight on the sensing mechanism in polyethylene glycol diacrylate/gold nanocomposite optical transducers. *Heliyon* **10**, e25593 (2024).
41. Pullagura, B. K., Amarapalli, S. & Gundabala, V. Coupling electrohydrodynamics with photopolymerization for microfluidics-based generation of polyethylene glycol diacrylate (PEGDA) microparticles and hydrogels. *Colloids Surf. Physicochem Eng. Asp.* **608**, 125586 (2021).
42. Alshamrani, M., Ayon, N. J., Alsalhi, A. & Akinjole, O. Self-Assembled nanomicellar formulation of docetaxel as a potential breast Cancer chemotherapeutic system. *Life* **12**, 485 (2022).
43. Zhou, W. et al. Preparation of calcium alginate/polyethylene glycol acrylate double network fiber with excellent properties by dynamic molding method. *Carbohydr. Polym.* **226**, 115277 (2019).
44. Lee, B. B., Ibrahim, R., Chu, S. Y., Zulkifli, N. A. & Ravindra, P. Alginate liquid core capsule formation using the simple extrusion dripping method. *J. Polym. Eng.* **35**, 311–318 (2015).
45. Chan, E. S. Preparation of Ca-alginate beads containing high oil content: influence of process variables on encapsulation efficiency and bead properties. *Carbohydr. Polym.* **84**, 1267–1275 (2011).
46. Lee, B. B., Ravindra, P. & Chan, E. S. Size and shape of calcium alginate beads produced by extrusion dripping. *Chem. Eng. Technol.* **36**, 1627–1642 (2013).
47. Belhouchat, N., Zaghouane-Boudiaf, H. & Viseras, C. Removal of anionic and cationic dyes from aqueous solution with activated organo-bentonite/sodium alginate encapsulated beads. *Appl. Clay Sci.* **135**, 9–15 (2017).
48. Wang, X. et al. Core-shell alginate beads as green reactor to synthesize grafted composite beads to efficiently boost single/co-adsorption of dyes and Pb(II). *Int. J. Biol. Macromol.* **206**, 10–20 (2022).
49. Reig-Vano, B. et al. Structural and mechanical analysis on mannuronate-rich alginate gels and xerogels beads based on calcium, copper and zinc as crosslinkers. *Int. J. Biol. Macromol.* **246**, 125659 (2023).
50. Madaghiele, M. et al. Development of semi- and grafted interpenetrating polymer networks based on poly(Ethylene glycol) diacrylate and collagen. *J. Appl. Biomater. Funct. Mater.* **12**, 183–192 (2014).
51. Es-Haghi, H., Bouhendi, H., Marandi, G. B., Zohurian-Mehr, M. J. & Kabiri, K. Rheological properties of microgel prepared with long-chain crosslinkers by a precipitation polymerization method. *J. Macromolecular Sci. Part. B: Phys.* **51**, 880–896 (2012).
52. Mamaghani, K. R., Naghib, M., Zahedi, A., Rahmanian, M. & Mozafari, M. GelMa/PEGDA containing graphene oxide as an IPN hydrogel with superior mechanical performance. *Mater. Today Proc.* **5**, 15790–15799 (2018).
53. Jin, M. et al. The effect of gelma/alginate interpenetrating polymeric network hydrogel on the performance of porous zirconia matrix for bone regeneration applications. *Int J. Biol. Macromol* **242**, (2023).
54. Bertassoni, L. E. et al. Hydrogel bioprinted microchannel networks for vascularization of tissue engineering constructs. *Lab. Chip.* **14**, 2202–2211 (2014).
55. Liu, Y. et al. Effect of reactive time on flame retardancy and thermal degradation behavior of bio-based zinc alginate film. *Polym. Degrad. Stab.* **127**, 20–31 (2016).
56. Ronca, A. et al. A combined approach of double network hydrogel and nanocomposites based on hyaluronic acid and poly(ethylene glycol) diacrylate blend. *Materials* **11**, (2018).
57. Wan, Z., Wai Hin, L., Shegiwal, A. & Haddleton, D. Reversible bond formation via sulfur free reversible addition fragmentation in photo-3D printing. *Eur. Polym. J.* **196**, 112324 (2023).
58. Girón-Hernández, J., Gentile, P. & Benlloch-Tinoco, M. Impact of heterogeneously crosslinked calcium alginate networks on the encapsulation of β-carotene-loaded beads. *Carbohydr. Polym.* **271**, 118429 (2021).

Acknowledgements

This research was funded by the Ministerio de Ciencia e Innovación, grant number PID2020-116322RB-C32. This project has received funding from the European Union's Horizon 2020 research and innovation programme under the Marie Skłodowska-Curie grant agreement No. 713679. Yasmin Kabalan thanks Universitat Rovira i Virgili for a pre-doctoral contract (2021PMF-PIPF-24) within its Marti i Franquès programme.The authors acknowledge Dr. Rita Marimón Picó, Dr. Mariana Stefanova Stankova and Núria Argany Figueras for their help in ESEM analysis (Scientific & Technical Resources Service, Universitat Rovira i Virgili), while also thanking Dr. Esther Torrens Serrahima (Research technician, Department of Chemical Engineering, Universitat Rovira i Virgili) for her help in TOC experiments.

Author contributions

Y. K. carried out the experiments, processed and analyzed the experimental data. S. D. F. assisted Y. K. with conducting the DMA experiments, as well as with processing and analyzing the experimental data. Y. K. wrote the first version of the manuscript. B. T., M. G. and X. M. presented the idea, supervised the findings of this work and the project. B. T., M. G. and X. M. helped in the discussion of results, provided critical feedback and helped shape the research analysis, and manuscript. All authors reviewed and contributed to the final version of the manuscript.

Funding

This research was funded by the Ministerio de Ciencia e Innovación, grant number PID2020-116322RB-C32. This project has received funding from the European Union's Horizon 2020 research and innovation programme under the Marie Skłodowska-Curie grant agreement No. 713679. Yasmin Kabalan thanks Universitat Rovira i Virgili for a pre-doctoral contract (2021PMF-PIPF-24) within its Marti i Franquès programme.

Declarations

Competing interests

The authors declare no competing interests.

Additional information

Supplementary Information The online version contains supplementary material available at https://doi.org/10.1038/s41598-025-05352-y.

Correspondence and requests for materials should be addressed to X.M.

Reprints and permissions information is available at www.nature.com/reprints.

Publisher's note Springer Nature remains neutral with regard to jurisdictional claims in published maps and institutional affiliations.